Linear viscoelastic models
Part II. Recovery of the molecular weight distribution using viscosity data

Tommi Borg [a,*], Esko J. Pääkkönen [b]

[a] TomCoat Oy, Koskisenkuja 11, 62500 Evijärvi, Finland
[b] Tampere University of Technology, Laboratory of Plastics and Elastomer Technology, P.O. Box 589, 33101 Tampere, Finland

ARTICLE INFO

ABSTRACT

The constitutive models for the viscoelasticity of polymers are presented for determining molecular weight distributions (MWDs) from viscosity measurements. The inversion of this model derived from control theory and melt calibration procedure connects the relaxation modulus, viscosity, and other flow properties of a polymer. The linear principle enables simultaneous and accurate modelling of the relaxation modulus and of viscosity flow curves over a wide range. Starting from viscosity measurements, the new model is used to determine the MWD, linear viscoelastic relaxation moduli, and the relaxation spectra of polyethylene of different grades. In addition, two benchmark analyses of bimodal polystyrene are reported, and the capability of the model is proven by the two-box test of Malkin. The error of the modelled viscosity is smaller than that for previously reported models. One of the main features of this work is that no relaxation time or spectrum procedures were used to generate and model linear viscoelasticity.

© 2008 Elsevier B.V. All rights reserved.

1. Introduction

Bersted et al. made one of the most successful early attempts to find a relationship between the viscosity flow curve and molecular weight distribution (MWD), using the partition model [1–7]. The inverse problem of how to determine the MWD from viscosity was described by Malkin [8], and is known to be an ill-posed problem [9–16].

In our model, once the relation between the structure and measured data is set up, other properties are computed simultaneously on a frequency or time scale.

Our companion paper [17] presents the main concepts of the procedure, viscoelasticity, relationships to chain structures and dynamics, and the mathematical treatment by linear viscoelastic relaxation modulus. This paper presents the computations and results for the complex viscosity.

For a constant frequency it is misleading to use entangle and Rousean relaxations and relaxation times, since chain dynamics differ (as explained in Sections 2.1 and 2.2). We simply consider (mainly) elastic rheologically effective distribution (RED') $w'(\log \omega)$ and viscous RED'' $w''(\log \omega)$.

2. Theory

2.1. Modelling viscosity at different steady-state flow rates

We have developed a principle for using complex viscosity data obtained from a dynamic rheometer measured in the frequency-sweep mode. As described in the companion paper for the relaxation modulus, modern control theory as applied to dynamic systems can be used to derive the formulas for frequency rate ω and relations to distributions by the melt calibration. In this paper we use MWD as a function of frequency $w_i'(\omega) = w_i(M)$ from function of molecular weight M in which w_i is the weight fraction of component i in the mixture. Now the development procedure can be started from the principle $\eta*(\omega) = \sum w_i(M)\eta_i^*(\omega)$ as the sum of independent contributions according to Graessley [18] to get complex viscosity functional [19] for $\eta*(\omega) = \sum w_i(\omega)\eta_i^*(\omega)$.

The basic idea is to model steady impulses and the summed stress resulting from chain dynamics between molecules of different molecular sizes at a steady frequency rate ω. With the normalized rheologically effective distribution (RED), $w(\omega)$, and the impulse response, $h(\omega)$, we obtain system response $y(\omega)$ according to control theory as follows:

$$y(\omega) = \int_{-\infty}^{\omega} w(\psi)h(\omega - \psi)\, d\psi. \tag{1}$$

As the MWD function is normally a function of logarithmic variables, or here RED $w(\log \omega)$, we have to rewrite all variables and

* Corresponding author.
E-mail address: tommi.borg@tomcoat.com (T. Borg).

Nomenclature

Hf	conversion factor between M and ω scales
$M(\omega)$	calibration curve for melts
Mf	structural value
Mf_0	structural value at the reference temperature
P'	elasticity value
P''	viscosity value
R	ratio of effective distribution ranges
$w'(\omega)$, $w'(\log \omega)$	rheologically effective distributions, (elastic) RED′
$w''(\omega)$, $w''(\log \omega)$	rheologically effective distributions, (viscous) RED″
$w'_c(\omega)$, $w'_c(\log \omega)$	characteristic effective distributions, (elastic) RED
ω_c	characteristic frequency
η_c^*	characteristic complex viscosity
%RMSE	percentage root-mean-square error function between observed and fitted viscosity curves

functions in Eq. (1) on a logarithmic scale: $\log \omega - \log \psi = \log(\omega/\psi)$, and $d\psi$ is written as $d(\log \psi)$. System response $y(\log \omega) = \log(\eta*(\omega)/\eta_0^*)$ is a normalized complex viscosity η^* with zero viscosity η_0^*. We can rewrite the presented complex viscosity functional for the normalized complex viscosity in the steady frequency rate as follows:

$$\log \frac{\eta*(\omega)}{\eta_0^*} = -P' \int_{-\infty}^{\log \omega} w(\log \psi) \left(\log \frac{\omega}{\psi} \right) d \log \psi. \tag{2}$$

We use entanglement relaxation modulus and Rouse relaxation and the respective REDs to illustrate the procedure. Complex viscosity $\eta^*(\omega)$ has a different physical origin and chain dynamics at a steady frequency. At higher steady frequencies, an oriented and disentangled chain tries to relax and re-entangle, conforming mainly to constant stress with an elastic response according to RED′ $w'(\log \omega)$. At very low steady frequencies, molecular friction generates mainly constant stress with a viscous response according to RED″ $w''(\log \omega)$. During the constant state it is misleading to use entangling and Rousean relaxations; instead we simply consider (mainly) elastic RED′ $w'(\log \omega)$ and viscous RED″ $w''(\log \omega)$ over the normal data measurement range. The complete formula for $\eta^*(\omega)$ at different frequencies can be expressed by common logarithmic distributions as

$$\log \frac{\eta*(\omega)}{\eta_0^*}$$
$$= - \int_{\log \omega/T}^{\log \omega} \left(P'w'(\log \psi) + P''w'' \left(\log \frac{\psi}{R} \right) \right) \log \frac{\omega}{\psi} d \log \psi. \tag{3}$$

where scalar values P' and P'' are elastic and viscous constants, respectively. This is achieved simply by copying function $w'(\log \omega)$ after dividing ω by the ratio, R, of the frequency-rate ranges to obtain the distribution, $w''(\log(\omega/R))$, if better information is not available. Viscous RED″ $w''(\log(\omega/R))$ is outside the range of standard viscosity measurements, but at very low frequencies ω also has elastic effects. During steady-state frequency, the longest chains are no more effective for the viscosity and we have to use the lower bound of integration $\log \omega - \log T = \log(\omega/T)$ instead of the minus infinity limit. The sampling band is still wide in the range $T = 100{,}000/s$ for polydisperse polymers.

The model described by Eq. (3) includes complex viscosity $\eta^*(\omega)$ without difficulty, but solving distribution $w'(\omega)$ is known to be a severely ill-posed problem.

2.2. Conversion from the distribution $w(\omega)$ to $w(M)$ (MWD) by melt calibration

When an effective distribution function (RED′) $w'(\log \omega)$ is found from the best fit to the viscosity, we must convert $w'(\log \omega)$ to a function of molecular weight, MWD $w(\log M)$, using a conversion factor between scale Hf and the polymer structural value Mf. The background of the melt calibration is presented earlier [17]; in the present paper we present the modelling of the steady shear conforming to a statistical orientated or stressed sphere linked to its midpoint.

The relation between the molecular weight scale M and the frequency scale ω is obtained using a homogeneous linear differential formula. The additional decrease in dM – converted by Hf on the M scale according to $- dM/d\omega$ – must equal the molecular weight scale divided by frequency M/ω:

$$Hf \frac{dM}{d\omega} + \frac{M}{\omega} = 0 \tag{4}$$

Solving Eq. (4) yields a simple relation for the melt calibration, $M(\omega)$, as a function of frequency, where the value of Mf is M at $\omega_1 = 1/s$:

$$M = Mf \left(\frac{\omega_1}{\omega} \right)^{1/Hf} \tag{5}$$

Conversions can be performed using a standard variable transformation as multivariate change-of-variable formula, Eq. (5), and the exponent (i.e. conversion factor between scales Hf and the polymer structural value Mf). MWD $w(M) = dW(M)/dM$, and $W(M)$ is the cumulative distribution of weight fractions of chains that, in the most-used semilogarithmic scale, is $w(\log M) = dW(M)/d(\log M)$. All distributions are normalized using an integral as for the following example for $w'(\log \omega)$:

$$\int_{-\infty}^{+\infty} w'(\log \omega) d \log \omega = 1 \tag{6}$$

The correct value of Mf for each polymer type is found by fitting data from gel-permeation chromatography (GPC) and size-exclusion chromatography (SEC), and dynamic measurements and models.

The inversion $\omega \propto 1/M$ generated from Eq. (5) is used in evaluations. High and low frequency rates correspond to small and large molecules, respectively. The calibration curves for melt (i.e. $M(\omega)$) may also be numerical function in practice.

2.3. Effective distribution $w(\omega)$ from viscosity measurements

We have to extract effective distribution $w'(\omega)$ from analytical Eq. (3), but solving this directly is known to be a severely ill-posed problem. Using a procedure similar to that described for the relaxation modulus, we obtain characteristic η_c^* for constant characteristic frequency ω_c as

$$\log \frac{\eta_c*(\omega)}{\eta_0^*}$$
$$= - \log \frac{\omega}{\omega_c} \int_{-\infty}^{\log \omega} \left(P'w'(\log \psi) + P''w'' \left(\log \frac{\psi}{R} \right) \right) d \log \psi \tag{7}$$
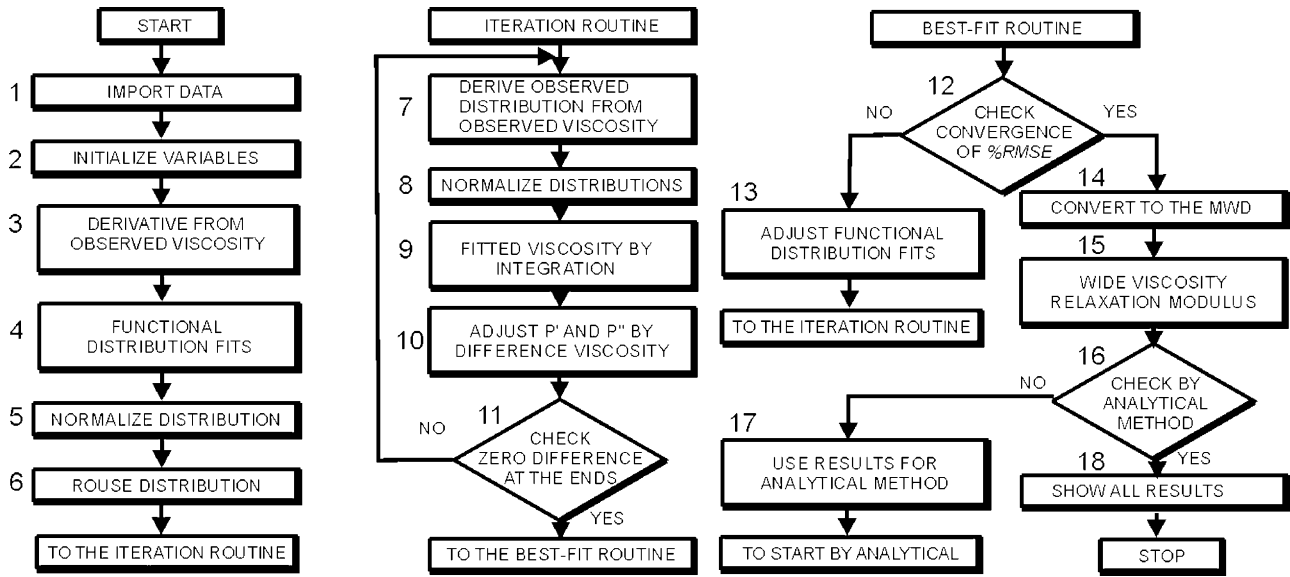
Fig. 1. Flowchart for the algorithm used to determine the MWD and the modelled viscoelastic properties.

To use viscosity measurements to detect the effective distribution, $w'(\omega)$, we have to solve Eq. (7) for RED′ function $w'(\log \omega)$ by deriving characteristic distribution $w'_c(\omega)$ as follows:

$$w'_c(\log \omega)$$
$$= -\frac{d}{d \log \omega} \frac{1}{P'} \left(\frac{\log(\eta * / \eta^*_0)}{\log(\omega/\omega_c)} + P'' \int_{-\infty}^{\log \omega} w'' \left(\log \frac{\psi}{R} \right) d \log \psi \right).$$
(8)

Normally, distribution $w'(\log \omega)$ and its copy $w''(\log(\omega/R))$ have zero or minimal overlap. This happens rarely with a broad MWD and a high polydispersity index ($MwR > 20$), but can be easily managed during the computation by performing the subtraction $w'(\log \omega) - w''(\log(\omega/R))$ before conversion for the output MWD. This overlapping situation differs from unentangled and entangled molecules found with the bimodal distribution discussed by Léonardi et al. [15,16], but may have an effect on the computed values of P' and P''.

2.4. Assumptions and limitations

The measured properties of a polymer are always described very accurately by RED $w(\omega)$ or $w(t)$, as derived from measurements according to Eq. (8) or computed solution from Eq. (3). The important question is whether or not the $w(M)$ generated by the melt calibration, computed by Eqs. (3) or (8), is correct. This can only be answered by making comparisons of the derived MWD with values from other procedures, such as GPC, as is done in Section 4. There is a major problem in such comparison work: GPC/SEC works well with soluble polymers, such as polystyrene (PS), but may exhibit systematic errors when applied to polymers with low solubility, such as polyethylene (PE). Secondary PE contains very long and thin molecules, and during shear the modelled statistical effective sphere may tend toward the statistical plane direction, as indicated by the detected value of $Hf = 2.05$ differing from the common value of $Hf = 4$ for many types of polymer.

We can measure viscosity only over a limited frequency range, but this can be extended using our models. The accuracy of the method deteriorates as the true polydispersity of the MWD increases. Master curves for viscosity generated by time–temperature superposition conversions have distortion points for derivations at junction points of different temperatures, as shown below with PS samples.

3. Numerical methodology

3.1. Computation description

The principal algorithm used to implement the presented formulas is described on a step-by-step basis based on the measured complex viscosity data η^*_{obs} as shown in the flowchart in Fig. 1.

As indicated in Fig. 1, the computation is performed in three phases: initialization, iteration, and best-fit routines. The initialization routine involves the following steps:

1. Measured complex viscosity data (η^*_{obs}) is imported from the database.
2. Initial values are given for structural factor Mf and the relation exponent for the Hf scales, and random values are used for elasticity P' and the viscous P'' factor.
3. The observed η^*_{obs} data are solved according to Eq. (8) by obtaining the observed characteristic effective distribution RED′$_{obs}$ $w'(\log \omega)_{obs}$ segment. During the derivation there is a discontinuity at ω_c, which must be omitted.
4. Distribution-segment fits to $w'(\log \omega)_{fit}$ are approximated on both sides of the $w'(\log \omega)_{obs}$ curve. The procedure can be performed by extrapolating from $w'(\log \omega)_{obs}$ lines, fitting the normalized distribution with $w'(\log \omega)_{obs}$, or using a priori information for the MWD. When the MWDs are narrow compared to the respective frequency range, segment fits do not have any effect since $w'(\log \omega)_{fit} = 0$.
5. The RED′ $w'(\log \omega)$ is normalized.
6. The RED″ distribution $w''(\log(\omega/R))$ is generated simply by copying RED′ $w'(\log \omega)$, if better information is not available.

3.2. Iteration process

The iteration routine involves the use of several loops to accurately fit the modelled viscosity with that measured at the lowest and highest frequencies:

7. The η^*_{obs} data are solved according to Eq. (8) to generate $w'(\log \omega)_{obs}$.
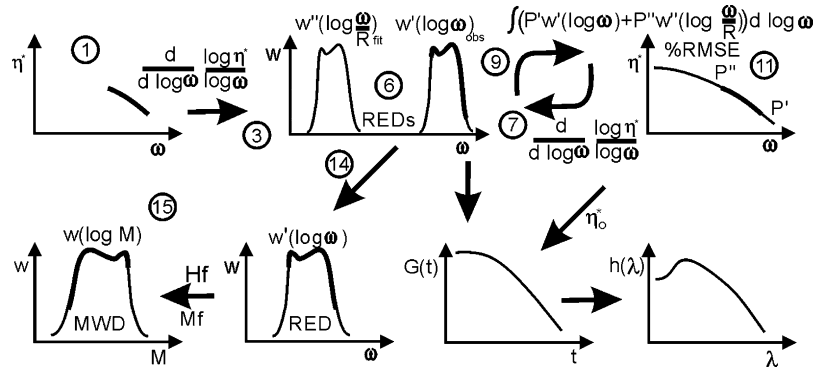
Fig. 2. Data flowchart of the procedure. Direct results are shown by thicker lines on log scales, except for the *w* scale, and the thinner lines are the modelled values. Numbers inside circles correspond to the steps in Fig. 1.

8. Distributions RED′ $w'(\log \omega)$ and $w''(\log(\omega/R))$ are normalized.

9. The wide-range fit η^*_{fit} is calculated from $w'(\log \omega)$ and $w''(\log(\omega/R))$ by integrating according to Eq. (7).

10. The values of P' and P'' are adjusted by a bracketing procedure to reduce the values of the lowest and highest frequency points of the difference viscosity curve ($\Delta\eta_* = \eta^*_{\text{obs}} - \eta^*_{\text{fit}}$) to zero within an assigned error.

11. This iteration loop is performed until the highest and lowest data points are equal to the modelled viscosity values, or numerically $\Delta\eta^* = 0$ at those points.

3.3. Fitting routines

Least-square procedures are widely used in numerical computations. Here the quality of the fit between the observed η^*_{obs} and predicted η^*_{fit} viscosity values was quantified using a modified least-square procedure called the percentage root-mean-square error function (%RMSE) [20]:

$$\%\text{RMSE} = \frac{100}{N}\sqrt{\sum_{i=1}^{N}\left(\frac{\eta^*_{\text{obs}} - \eta^*_{\text{fit}}}{\eta^*_{\text{obs}}}\right)^2} \qquad (9)$$

where N is the number of data points:

12. The best-fit routine is used to find the smallest error (based on the %RMSE value) between viscosity measurements and the modelled viscosity.

13. Convergence of the %RMSE value is checked so as to find the minimum of all %RMSE values obtained during iterations.

14. If there is still a chance to find a better fit, iterations are continued after slightly adjusting the distribution-segment fit $w'(\log \omega)_{\text{fit}}$ for the new position, and again applying the iteration routine to obtain the RED′.

15. When the best fit is found, we convert $w'(\log \omega)$ to the final MWD $w(\log M)$ using *Mf* and *Hf* values by the melt-calibration concept according to Eq. (5).

16. Check if the analytical method described by Eq. (3) has already been used.

17. Convert constants used in the analytical method into a new complete loop, using the same procedure as for the characteristic method as much as possible. This improves the likelihood of solving analytical Eq. (3) to obtain the RED′ and MWD with standard solution methods based on a priori information using parallel computing.

18. Show and compare results obtained from both the fast integral (Eq. (8)) and analytical (Eq. (3)) methods.

Also, wide-range and accurate viscosity fits and relaxation modulus $G(t)$ are computed [17], and spectrum $h(\lambda)$ is computed according to Eq. (10). Fig. 2 shows the results.

The structural and conversion factors (*Mf* and *Hf*) between scales are found for new polymer types by comparing the results obtained with GPC and SEC. *Mf* and *Hf* influence only the average molecular weight $\bar{M}_{\text{w}}$ and *MwR*, respectively. A segment of the distribution related to the MWD is gained directly by
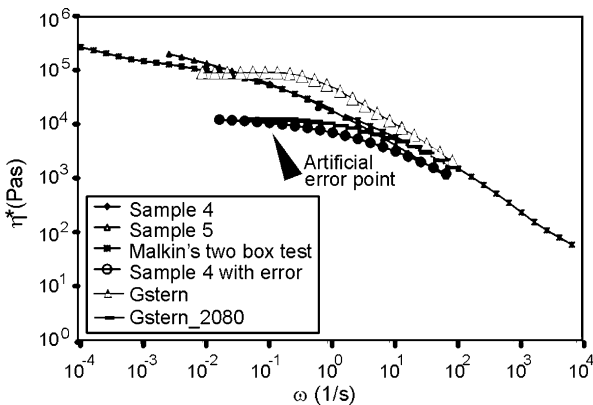

Fig. 3. Complex viscosity of Borealis HDPE Sample 4, Sample 5, fictional Malkin's two-box test and Sample 4 with artificial error point. The data were used to compute MWDs for Figs. 4–6, 9 and 10.
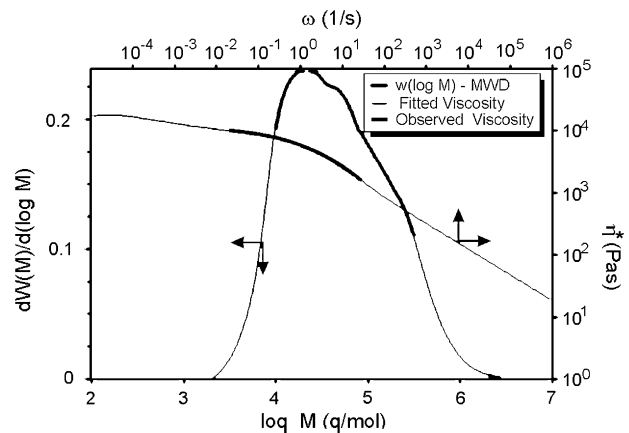

Fig. 4. MWD curve for Borealis HDPE Sample 4. The thicker segment of the MWD curve has been computed directly from viscosity data by derivation. The viscosity curves are also shown for measured (thick) and computed (thin) segments.
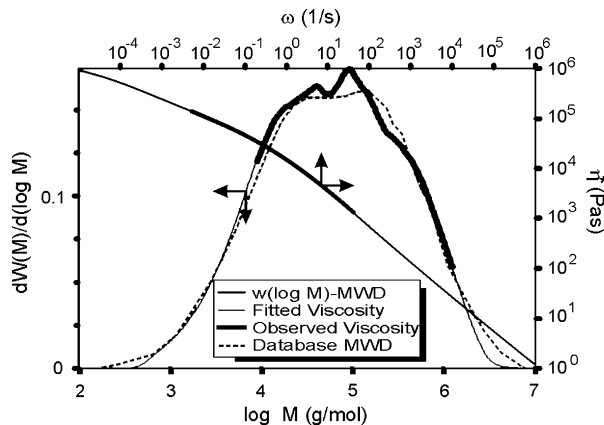
Fig. 5. MWD curve for Borealis HDPE Sample 5. The received GPC data are labelled as "Database MWD" on the chart. The viscosity curves are also shown for measured (thick) and computed (thin) segments.

derivation from the measured data, and then several rheological properties are computed by integrating the derived and modelled distributions.

The formulas contain a variable in the exponent, and hence in the numerical computation practice we need to consider logarithmic and exponential functions simultaneously during cyclic derivation, integration, and for other computations – this power-integral-logarithm-derivation processing is a very unstable technique due to the presence of some difference between the measurements and the model values. We therefore adapted the standard numerical methods found in textbooks for this case.

3.4. Relaxation spectrum

The relaxation spectrum $h(\lambda)$ can be approximated by deriving relaxation modulus $G(t)$ according to the procedures presented by Tschoegl [21]. The following equation is an example of how to obtain $h(\lambda)$ using up to the third derivative of $G(t)$:

$$h(\lambda) = -\frac{dG(t)}{d \log t} + \frac{3d^2 G(t)}{2(d \log t)^2} - \frac{d^3 G(t)}{2(d \log t)^3}|_{t=3\lambda} \tag{10}$$

3.5. Utilized software

The RheoPower software package comprises two separate software programs: (1) the RheoAnalyzer mode, which is used to find the MWD from viscosity or relaxation modulus curves; and (2) the RheoDeveloper mode, which is used to find modelled curves from structure. Both programs give simultaneous results

over broad ranges of viscosity, relaxation modulus, and spectrum fits.

Using the RheoAnalyzer program to find the MWD from viscosity data requires the viscosity flow curve as well as the values of *Mf* and *Hf*. The RheoDeveloper mode involves the following procedures:

1. Draw the MWD or import a data file.
2. Obtain factors *Mf* and *Hf* for a similar polymer using RheoAnalyzer.
3. Evaluate the values of *P'* and *P''*, and combine these with a single data point to produce the viscosity function.

3.6. Short computation history and set of equations

The development of the software for our programs has taken several years. We initially found Gleissle's [22] viscometric mirror relation ($\dot{\gamma} = 1/t$) very helpful, and the second generation of the software package was developed based on differential equations and rheological phenomena. The third generation of the software is compiled in fluent binary form, and can complete the computation in minutes when running on a standard PC. In contrast, computations using the first version of the software required hours or even days.

4. Experimental

4.1. Procedure and test polymers

All of the computations were performed using components of the software package running on a standard PC with the characteristic model except where stated otherwise, since a detailed presentation and comparison of the results from the analytical model is beyond the scope of this article. The computation is performed after first importing a data record into the databases and selecting *Mf* and *Hf*. It is well known that among polymers, detecting the MWD and modelling the rheology is most difficult for polyolefins. This is why we selected mainly high-density PE (HDPE) and low-density PE (LDPE) samples, although the procedure is now also very accurate for amorphous polymers such as PS.

Borealis Polymers kindly provided us with data of two HDPE samples: (1) a Ziegler–Natta catalyzed HDPE (coded as Sample 4 in this paper) and (2) a commercial grade HDPE (coded as Sample 5). Lupolen 1840H LDPE by BASF was adopted as the LDPE sample, since measured data were available and the material is widely reported in the literature. The sample was a modern version of the classical LDPE IUPAC A, or "Melt I", first reported by Meissner [23,24].
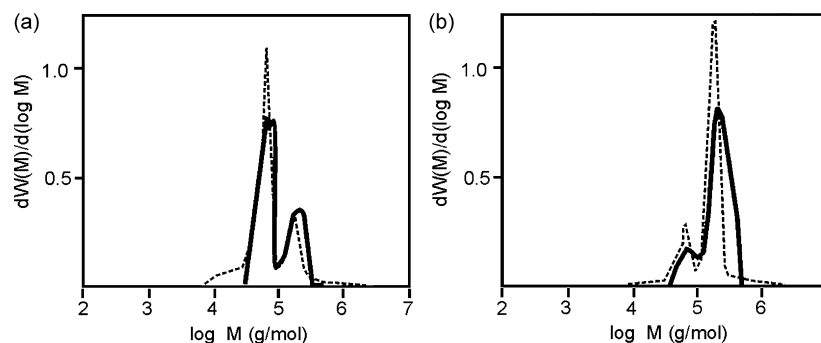

Fig. 6. PS benchmark test for workshop participants to carry out and present their own results from data: (a) "gstern_2080", describing a 20 wt% (177,000 g/mol PS) to a 20 wt% (60,000 g/mol PS) mixture of PS; and (b) "gstern" is an inverse mixture (ratio of 80:20). Dashed lines are data from GPC/SEC measurements.
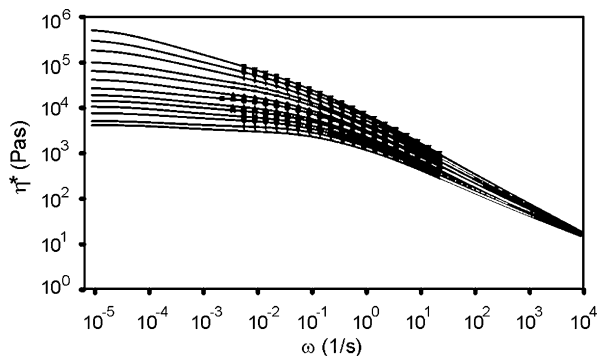
Fig. 7. Measured viscosity curves for Lupolen 1840H LDPE at temperatures ranging from 130 °C to 250 °C in 10 °C increments. The points are measured data provided by BASF, and the curves indicated over a wider scale were modelled by software. The average error (%RMSE) between the measured and modelled viscosities is 0.0009%.

PS samples were semi-blind data, in that their measurement manner and procedure, and origin and manufacturer were unknown. The data for two samples were received at a workshop, as explained below, and were simply marked "gstern_2080" and "gstern".

In the first stage we used data provided by the polymer manufacturer (HDPE) or data made for the benchmark at the workshop (PS), and in the second stage we used the data published in the literature compared with the data provided by the polymer manufacturer (LDPE). Finally, we performed two tests with fictional data to analyze the error sensitivity.

4.2. Measured viscosity data

Borealis Polymers gave us permission to use their HDPE viscosity data measured with a plate–plate rheometer. The company informed us that the data for Borealis Samples 4 and 5 were recorded by a strain-controlled device at a small strain amplitude and a temperature of 190 °C. The data are shown in Fig. 3.

BASF gave us permission to use their oscillating-rheometer data for Lupolen 1840H LDPE, measured at temperatures from 130 °C to 250 °C (see Fig. 7). The main characteristics of these samples are listed in Table 1.

4.3. Constants

Only two polymer-dependent constants are used. For the HDPE sample, Mf was 52,900 g/mol at 190 °C and the default set of $R = 10^6$ was set for the distance for the ratio of effective distribution ranges. The bimodal HDPE (Sample 5) exhibits exceptional polymerization, and thus it has $Mf = 70,000$ g/mol. An ex For the LDPE sample, $Mf = 37800$ g/mol at 150 °C was used. The relation scale exponent for PE, $Hf = 2.05$, was held constant for all polyolefin cases. For comparison, the respective constants for PS were $Mf = 136,000$ g/mol and $Hf = 4$. Please note that the values P' and P'' were obtained using the viscosity-fitting procedure, with no ad hoc constants or values being used.

A constant characteristic frequency of $\omega_c = 1/s$ or the mean value of the highest and lowest measured frequencies, and a constant characteristic time of $t_c = 10^{-6}$ s was used for relaxation simulations.

4.4. MWD from HDPE viscosity data

Fig. 4 shows the measured MWD for Borealis Sample 4. The thicker segment of the MWD curve was computed by derivation directly from the viscosity data, which is a well-posed result as shown by comparison with the original measured viscosity. The modelled wide-range fitted-viscosity curve and the earlier known-MWD curve are still mildly ill-posed, meaning that the amounts of low and high fractions are not accurate even though the computation is stable. In summary, the generation of this chart required the simultaneous application of computing and modelling for MWD, and modelling of the wide-range viscosity curve from the developed MWD, as described in Section 3. Using the viscosity data of Borealis Sample 4, our computation (from rheological properties to MWD) procedure produced $\bar{M}_w = 113,000$ g/mol and $MwR = 5.9$.

The respective values obtained from GPC measurements for Sample 4 were $\bar{M}_w = 132,000$ g/mol and $MwR = 4.1$, which indicates that the error was at the level of numerical errors (with

Table 1
Main characteristics of all investigated samples and computations

	T[a]	M_w[b]	M_w/M_n[b]	Mf[c]	Hf[c]	P'[d]	P''[d]	%RMSE[e]
Part I: Fig. 3b		100 000	1.2	37 800	2.05	0.10	0.10	
LDPE IUPAC A	150	480 000	25.0	37 800	2.05	0.38	0.20	
Part II: HDPE Sample 4	190	113 000	5.9	52 900	2.05	0.40	0.10	0.0014
HDPE Sample 5	190	224 000	17.4	52 900	2.05	0.30	0.40	0.0015
PS gstern_2080	170	99 118	1.4	136 000	4	0.39	0.08	0.0030
PS gstern	170	170 615	1.3	136 000	4	0.56	0.16	0.0037
LDPE Lupolen 1840H	130	214 404	13.3	32 508	2.05	0.21	0.43	0.0011
LDPE Lupolen 1840H	140	235 996	14.3	35 532	2.05	0.28	0.38	0.0007
LDPE Lupolen 1840H	150	239 973	14.6	37 800	2.05	0.26	0.39	0.0011
LDPE Lupolen 1840H	160	238 833	14.2	40 068	2.05	0.28	0.35	0.0007
LDPE Lupolen 1840H	170	239 191	14.3	42 092	2.05	0.32	0.32	0.0007
LDPE Lupolen 1840H	180	239 505	14.1	45 360	2.05	0.35	0.29	0.0007
LDPE Lupolen 1840H	190	239 580	14.4	47 628	2.05	0.35	0.27	0.0007
LDPE Lupolen 1840H	200	237 497	14.0	50 652	2.05	0.37	0.25	0.0007
LDPE Lupolen 1840H	210	240 150	14.2	52 920	2.05	0.38	0.25	0.0007
LDPE Lupolen 1840H	220	215 824	13.5	55 188	2.05	0.41	0.21	0.0011
LDPE Lupolen 1840H	230	236 195	14.4	57 456	2.05	0.34	0.24	0.0012
LDPE Lupolen 1840H	240	239 123	14.3	60 748	2.05	0.45	0.17	0.0011
LDPE Lupolen 1840H	250	203 579	12.5	62748	2.05	0.41	0.16	0.0015
Fictional Two-box		256 000	17.0	70 000	2	0.30	0.32	0.0380

[a] Measured temperature in Celsius °C.
[b] Computed average molecular weight M_w in g/mol and polydispersity index M_w/M_n.
[c] Used structural value Mf and conversion factor Hf. Information not always available, if the used rheometer type was plate-plate or cone-plate.
[d] Obtained or used elasticity and viscosity values P' and P''.
[e] Obtained percentage root-mean-square error function %RMSE.
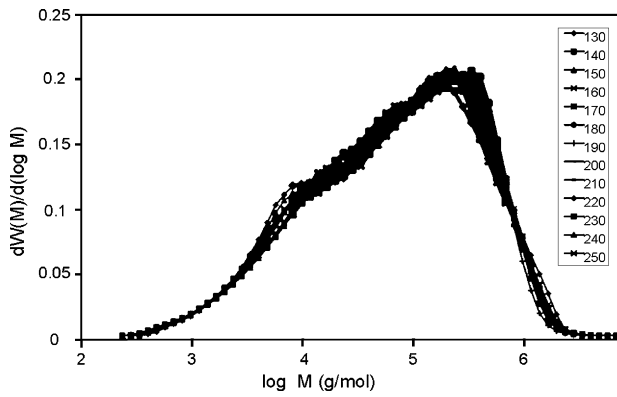
Fig. 8. Summary of Lupolen 1840H LDPE MWDs computed from data measured at temperatures from 130 °C to 250 °C (in 10 °C increments). The deviation in $\bar{M}_w$ was 2.3%, indicating that the procedure was repeatable.

%RMSE = 0.0014%). It is known that GPC measurements are comparative (i.e. absolute values cannot be obtained), and become less accurate for higher molecular weight (HMW) fractions.

Fig. 4 shows the computed MWD for Borealis Sample 5. The viscosity values are shown for measured (thick) and computed (thin) segments.

For Fig. 5 (Sample 5), we also received GPC data from Borealis, labelled "Database MWD" in the chart. GPC showed $\bar{M}_w$ = 280, 000 g/mol and MwR = 22.2, and the software produced $\bar{M}_w$ = 224, 000 g/mol and MwR = 17.4, indicating that the software did not overestimate the HMW fractions.

An interesting observation is the bimodal shape of the MWD curve, which is especially evident in Fig. 5. The MWD data has a bimodal shape according to GPC measurements, and this was also reproduced in our computations.

The rheological method appears to be more sensitive than GPC/SEC chemical methods for detecting bimodal MWDs. No system smoothing was evident when GPC devices were used to measure the MWD for PS, but with PE there appeared to be significant smoothing coming from the procedure. We found that GPC smoothed more as our characteristic method based on derivation from viscosity data.

4.5. Benchmark tests for PS

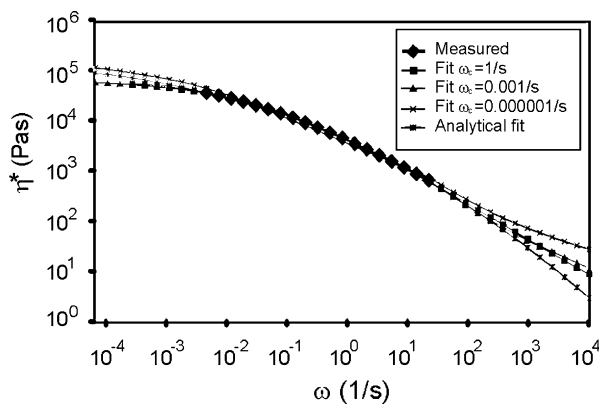The organizers of the "Second Workshop on Inverse Problems in Rheology and Related Experimental Techniques", held in Germany during May 9–11, 2001, arranged a public benchmark test for participants to carry out and present their own results. The organizers provided information as distribution charts measured by GPC on the MWDs, but the manufacturer remained unknown. We extracted PS data from G' and G'' master curves to develop η^* as arranged by the organizers. According to the parameters of the benchmark test, no other information on the measuring procedure was available, but the organizers did reveal that the given MWDs were measured chemically. We show two bimodal results of samples "gstern_2080" and "gstern" in Fig. 6. These narrow – but still bimodal – MWD results are wholly analytical according to characteristic model: chemically measured MWDs are indicated by dashed lines as given in the MWD forms distributed by the workshop organizers.

This test not only demonstrated the capability of detecting bimodality of both samples, but also showed that the generated master curves in the range 0.01/s < ω < 100000/s have severe errors in the joint points of different temperatures. For the complete master curve, the error was very high, at %RMSE = 0.5000%, and for "gstern" it was %RMSE ≈ 2%. We had to narrow the data range for the computation to reduce the error, because the data were probably measured at a single temperature over this frequency range. Thus, the used frequency range 0.06/s < ω < 100/s for "gstern_2080"

Fig. 10. Fictional Malkin two-box test. The viscosity curve was generated by the RheoDeveloper (MWD-Pro, i.e. from MWD to the properties) software, starting from the data labelled "Original MWD". The viscosity scale is arbitrary, but the relative changes are in agreement with the theory. Using the generated viscosity curve, the MWD results shown here were generated again using RheoAnalyzer (Pro-MWD). The recalculated fitted MWD is very close to the original MWD, with differences only evident at the peaks.

Fig. 9. Effects of characteristic frequency ω_c on viscosity obtained using the characteristic model, measured data for ω in the range from 0.007/s to 3/s at 150 °C, and analytical fits of Lupolen 1840H LDPE. All simulations are accurate within the measurement range except for ω_c = 0.000001/s.
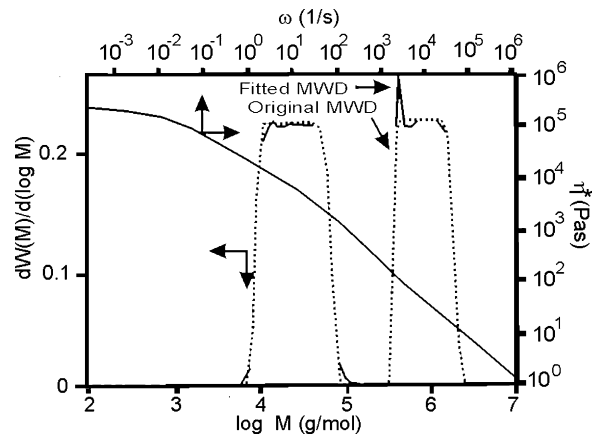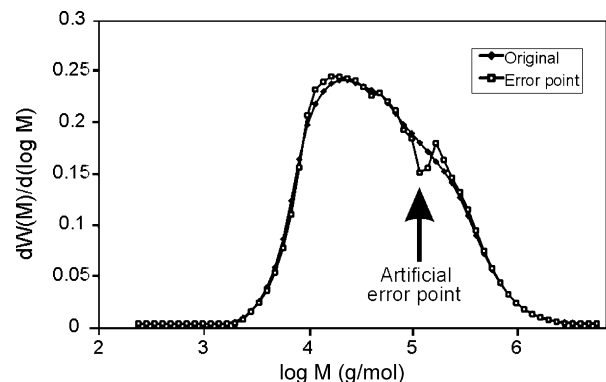

Fig. 11. Simulation test for the MWD shows how a small (1%) error in a single viscosity data point can distort the MWD curve of Sample 4 (shown in Fig. 3). An artificial frequency error of 0.1/s was added to the viscosity.

gave %RMSE = 0.0030% and for "gstern" the range 0.02/s < ω < 100/s gave the error %RMSE = 0.0037%. Therefore, the joint points of different temperatures in the master curve generate an error that is 100-fold larger, and hence they are not usable in this application.

With these narrow bimodal MWDs, we did not need to use filling MWDs at the sides or $w(\omega)_{\text{fit}} = 0$, and the complete relationship was analytically well-posed.

4.6. MWD from LDPE viscosity data

The viscosity of Lupolen 1840H LDPE measured at temperatures from 130 °C to 250 °C is shown in Fig. 7, where the points are measured data provided by BASF. The wide-range modelled viscosity curves are based on computations.

The MWDs of LDPE computed at 13 temperatures are summarized in Fig. 8. This test revealed that temperature had a minor effect on the values of the constants:

$$Mf = Mf_0 + (T - T_0) \times 250.$$

For LDPE, Mf_0 was 47,600 g/mol at 190 °C, as for HDPE was Mf = 52,900 g/mol at 190 °C, and at 250 °C Mf for LDPE was 62,600 g/mol. We found that the average error between the measured viscosity data and the model was %RMSE = 0.0009%, which is more than 50 times smaller than that for any other published model.

The average $\bar{M}_w$ was 235,000 g/mol (with a deviation of 2.3%) and MwR = 14.1 for all computations.

The effects of different values of characteristic frequency ω_c are shown in Fig. 9. Within the measurement range, the modelled analytical and characteristic values are very similar to the measured values. Since we cannot measure very high and low frequencies, the figure includes some estimated values. Moreover, there are minimal differences between the analytical and characteristic models for $\omega_c > 0.0001$/s, and the optimal value for ω_c can be found by fitting procedures.

4.7. Malkin's two-box test

The two-box test by Malkin [8] was used to simulate transformations from the MWD to the viscosity flow curve, and vice versa. The RheoDeveloper software was first used to draw two cubic boxes, simulating bimodal MWDs. The computed viscosity curve
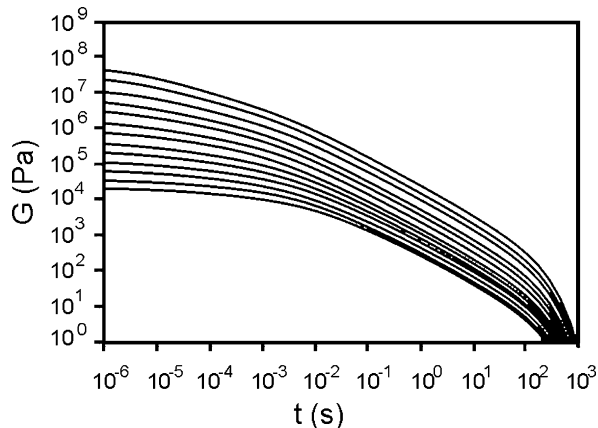

Fig. 13. Relaxation moduli of Lupolen 1840H LDPE at temperatures from 130 °C to 250 °C (in 10 °C increments).

was saved in the databases and used by the RheoAnalyzer software. The results are shown in Fig. 10, which indicates the generation of minimal noise that only slightly distorts the MWD boxes. The source of the noise is known and coming from tuned derivation, but the software is for practical computations. Moreover, $\bar{M}_w$ and MwR are close to their original values.

4.8. Simulation of sensitivity to data error

A simulation test was performed to determine the effect of a small (i.e. 1%) error in the viscosity data point on the MWD results. Taking the measured viscosity data of Borealis Sample 4 used in Fig. 11, we generated an artificial 1% viscosity error at a frequency of 0.1/s, by changing the originally measured η from 8798 to 8886 Pas. On a logarithmic scale, this changed the data point from 3.9444 to 3.9487, which was impossible to detect visually on the flow curve.

Fig. 11 shows that the computed MWD exhibits significant distortion on the HMW side, with %RMSE increasing from 0.0013% to 0.0018%. It must also be borne in mind that even more severe errors are caused by measuring-system deviations such as slipping, poor mixing of compounds, or poor relaxation of the sample. The error evaluation shows that it is impossible to detect the MWD from a manually copied viscosity curve. In this method, moderate absolute errors can be present in the viscosity, but the relative errors must be minimal.
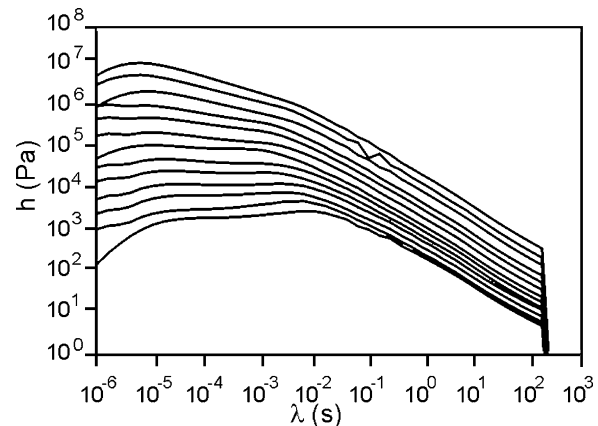

Fig. 12. Typical %RMSE errors for different known models compared to the computation levels for modelled viscosity curves. "Records" indicates errors in data, "Models" compares different models for viscosity curves and "RheoAnalyzer" relates to data assurance. Our method is more than 100 times more accurate than other models at modelling viscosity curves.

Fig. 14. Relaxation spectra of Lupolen 1840H LDPE at temperatures ranging from 130 °C (top curve) to 250 °C (bottom curve) (in 10 °C increments).
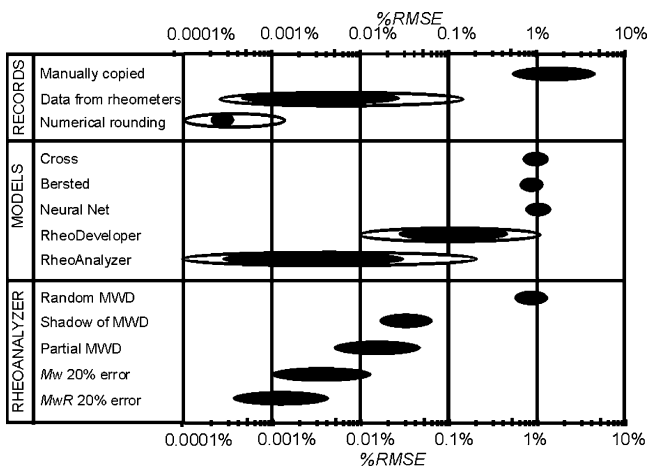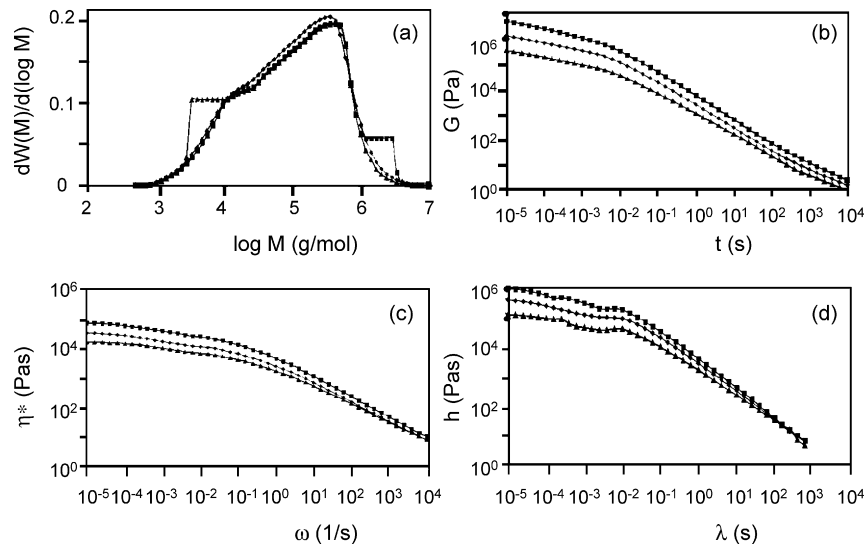
Fig. 15. What-if analyses for Lupolen 1840H LDPE at 190 °C reveals large changes in modelled viscosity, relaxation modulus, and spectrum. (a) Small differences are evident in the cubic shape of the MWD. Original values of $\bar{M}_w$ and polydispersity MwR are 230,000 g/mol and 11, respectively. $\bar{M}_w$ = 202, 000 g/mol and MwR = 11.7 for the left-side cubic bump, and $\bar{M}_w$ = 296, 000 g/mol and MwR = 11.0 for the right-side bump. (b) Relaxation modulus $G(t)$. The maximal relaxation time is not set for the spectrum maximal relaxation time, and the maximal relaxation time is not used so as to demonstrate the cross-point of the spectrum in Fig. 15d. (c) Modelled shear viscosity η starting from MWD (modelled here as complex viscosity η^*). (d) Modelled relaxation spectrum $h(\lambda)$.

4.9. Evaluation of error

The calculation of the MWD is extremely sensitive to errors in the recorded data. The influences of error sources and the precision of records on the estimation are summarized in Fig. 12.

De Vries et al. [20] used %RMSE values of viscosity for the well-defined metallocene-based molecular structures of polyolefin elastomers and plastomers. Their shear-rate range was $0.1/\text{s} < \omega < 10000/\text{s}$. The values for %RMSE were in the range 0.6–1.3% for the model of Bersted et al. and 0.8–1.5% for the cross-model; in their (1996) neural net model, %RMSE was in the range 1.2–2.5%.

A simple test revealed that it was possible to copy viscosity values manually to a precision level of log 0.01, resulting in an %RMSE on the order of 0.5%. The values of %RMSE for our first- and second-generation software were in the ranges 0.5–0.05% and 0.05–0.01%, respectively, and is currently in the range 0.0040–0.0003%. In most computation cases we must omit data values for less than $\omega = 0.001/\text{s}$ and records with a range giving increased %RMSE values.

Whilst Fig. 12 lists some typical calculated %RMSE values, the relative errors were generally much smaller during measurements. The error for the torque resolution of rheometers is typically less than 0.1%, which results in a %RMSE of the viscosity flow curve of 0.023%. Numerical rounding errors typically produce a %RMSE of 0.0013%.

4.10. Modelling relaxation modulus and spectrum

The computed relaxation modulus, $G(t)$, is not subject to terminal or instrumentation limitations. We set the spectrum maximal relaxation time, $\lambda_{\max}$, to 400 s.

The wide-range relaxation moduli and relaxation spectra curves for Lupolen 1840H LDPE computed at 13 temperatures are shown in Figs. 13 and 14, respectively. These curves are smooth, with only slight variations due to the sensitivity of the derivation.

4.11. What-if analyses

Other properties and the influence of changes in the MWD on the behavior can be simulated using what-if analyses. This enables the background of principle, where is possible to compute to the both directions (Fig. 15).

5. Conclusions

A new method for modelling viscoelasticity and polymer properties has been presented. The underlying mathematical technique is based on the modern control theory and the concept of melt calibration. In this study the method was used to determine the MWD from viscoelastic data, and vice versa. The results calculated from measured data confirmed that our model for determining the MWD from viscosity measurements works in practice, with the error being very small provided that the recorded data are accurate. The linearity principle makes it possible to model a wide range of linear viscoelastic relaxation moduli, provides a good and smooth approximation to the relaxation spectrum, and models viscosity flow curves simultaneously and accurately.

The major known limitation of the procedure is the narrow frequency range of the measured data. The accuracy of the method decreases when the MWD widens, or when the exponent in the relation for the Hf scales becomes higher. As mentioned [17], polyolefin is a difficult material (Hf = 2.05), whereas PS is easy (Hf = 4). The linearity principle allows data from different sources to be combined, which should be expanded upon. The attractive subject of long chain branching and other fields, as well as different polymer types need to be investigated more thoroughly.

The characteristic method presented in this paper is rapid and versatile, and could be used in the quality control of a polymerization process or as a design aid in simulations, for example. The calculation software could also be used in reverse to calculate MWDs at higher values, where GPC/SEC measurements are problematic, or used in parallel with other methods to enhance their accuracy. The results for the analytical model demonstrate its usefulness as a tool for investigating the microstructure. We are continuing to develop characteristic and analytical models for parallel computations, and are comparing different procedures to obtain practical outputs.

The examples shown here have focused on detecting chemical structure distributions of homogeneous polymer melts, but

effectively determining the distributions for rheological properties (RED′) ($w'(\omega)$) is more important in practical processing applications and for enabling the simulation of flow properties that are impossible to measure.

The method is applicable to solutions, and even biopolymers. Whilst the underlying principle is simple, the use of the numerically sensitive and labile recursive exponent formulas require accurate data together with fluent software to achieve high computing accuracy.

Acknowledgments

References

[1] B.H. Bersted, An empirical model relating the molecular weight distribution of high-density polyethylene to the shear dependence of the steady shear melt viscosity, J. Appl. Polym. Sci. 19 (1975) 2167–2177.

[2] B.H. Bersted, A model relating elastic properties of high-density polyethylene melts to the molecular weight distribution, J. Appl. Polym. Sci. 20 (1976) 2705–2714.

[3] B.H. Bersted, Prediction of dynamic and transient rheological properties of polystyrene and high-density polyethylene melts from the molecular weight distribution, J. Appl. Polym. Sci. 23 (1977) 1279–1289.

[4] B.H. Bersted, J.D. Slee, A relationship between steady-state shear melt viscosity and molecular weight distribution in polystyrene, J. Appl. Polym. Sci. 21 (1977) 2631–2644.

[5] B.H. Bersted, Effect of molecular weight distribution on elongational viscosity of undiluted polymer fluids, J. Appl. Polym. Sci. 24 (1979) 671–682.

[6] B.H. Bersted, J.D. Slee, C.A. Richter, Prediction of rheological behavior of branched polyethylene from molecular structure, J. Appl. Polym. Sci. 26 (1981) 1001–1014.

[7] B.H. Bersted, On the effect of very low levels of long chain branching in rheological behavior in polyethylene, J. Appl. Polym. Sci. 30 (1985) 3751–3765.

[8] A.Ya. Malkin, Some inverse problems in rheology leading to integral equations, Rheol. Acta 29 (1990) 512–518.

[9] A.Ya. Malkin, A.E. Teishev, Flow curve-molecular weight distribution: is the solution of the inverse problem possible? Polym. Eng. Sci. 31 (1991) 1590–1596.

[10] W.H. Tuminello, N. Cudré-Mauroux, Determining molecular weight distributions from viscosity versus shear rate flow curves, Polym. Eng. Sci. 31 (1991) 1496–1507.

[11] M.T. Shaw, W.H. Tuminello, A closer look at the MWD-viscosity transform, Polym. Eng. Sci. 34 (1994) 159–165.

[12] Y. Liu, M.T. Shaw, W.H. Tuminello, Obtaining MWD information from the viscosity data of linear polymer melts, J. Rheol. 42 (1998) 453–476.

[13] Y. Liu, M.T. Shaw, W.H. Tuminello, Optimized data collection for determination of the MWD from the viscosity data of polymer melts, Polym. Eng. Sci. 38 (1998) 169–176.

[14] Y. Liu, M.T. Shaw, Investigation of the nonlinear mixing rule for its adequacy in viscosity to molecular weight distribution transforms, J. Rheol. 42 (1998) 267–279.

[15] F. Léonardi, A. Allal, G. Marin, Determination of the molecular weight distribution of linear polymers by inversion of a blending law on complex viscosities, Rheol. Acta 37 (1998) 199–213.

[16] F. Léonardi, A. Allal, G. Marin, Molecular weight distribution from viscoelastic data: the importance of tube renewal and Rouse modes, J. Rheol. 46 (2002) 209–224.

[17] T. Borg, E. J. Pääkkönen, Linear viscoelastic models. J. Non-Newtonian Fluid Mech (2008), doi:10.1016/j.jnnfm.2008.07.011.

[18] W.W. Graessley, Polymeric Liquids and Networks: Dynamics and Rheology, Garland Science, London, 2008.

[19] R.S. Anderssen, R.J. Loy, On the scaling of molecular weight distribution functionals, J. Rheol. 45 (2001) 891–901.

[20] S.A. de Vries, L.T. Kale, T. Oswald, T.P. Karjala, in: A. Aït-Kadi, J. Dealy, D. James, M. Williams (Eds.), Molecular structure—linear viscoelastic properties modeling for constrained geometry catalyst polyolefin resins, Proceedings of the XII International Congress on Rheology, Quebec, Canada, 18–23 August, 1996.

[21] N.W. Tschoegl, The Phenomenological Theory of Linear Viscoelastic Behavior: An Introduction, Springler-Verlag, Berlin/Heidelberg, 1989.

[22] W. Gleissle, in: G. Astarita, G. Marrucci, L. Nicolais (Eds.), Two simple time-shear rate relations combining viscosity and first normal stress coefficient in the linear and non-linear flow range, Proceedings of the 8th International Congress on Rheology, Naples 1980, Plenum Press, Rheology 2, p. 457.

[23] J. Meissner, Basic parameters, melt rheology, processing and end-use properties of three similar low-density polyethylene samples, Pure Appl. Chem. 42 (1975) 551–662.

[24] J. Meissner, Modifications of the Weissenberg rheogoniometer for measurement of transient rheological properties of molten polyethylene under shear. Comparison with tensile data, J. Appl. Polym. Sci. 16 (1972) 2877–2899.